MAGNET FOR THE PRINCETON-PENNSYLVANIA SYNCHROTRON

P. J. Reardon, L. Seidlitz, F. C. Shoemaker

(Presented by M. G. WHITE)

1. GENERAL CHARACTERISTICS

The C-shape for the Princeton-Pennsylvania Synchrotron [1] weak focusing magnet (Fig. 1) was chosen so that multiple experiments with small angle meson beams and several external proton beams would be feasible. The sixteen curved magnets, 3.7 m long at their outside radius, are separated by eight 2.14 m long straight sections; (Fig. 2) four for the RF stations, one for the inflector and three for the production of secondary beams, and eight 0.66 m long straight sections which serve both as pumping ports for the vacuum system and as locations of the electrostatic pick-up electrodes. The circumference of the orbit is 72 m and the radius of curvature of the equilibrium orbit is 9.14 m. The magnet is excited by a biased sine-wave at a frequency of 19 Hz with a minimum field of 260 Gs and a peak field of 14 kGs. The «*n*» is 0.58 uncorrected, the radial and vertical betatron wavelengths per revolution are 1.28

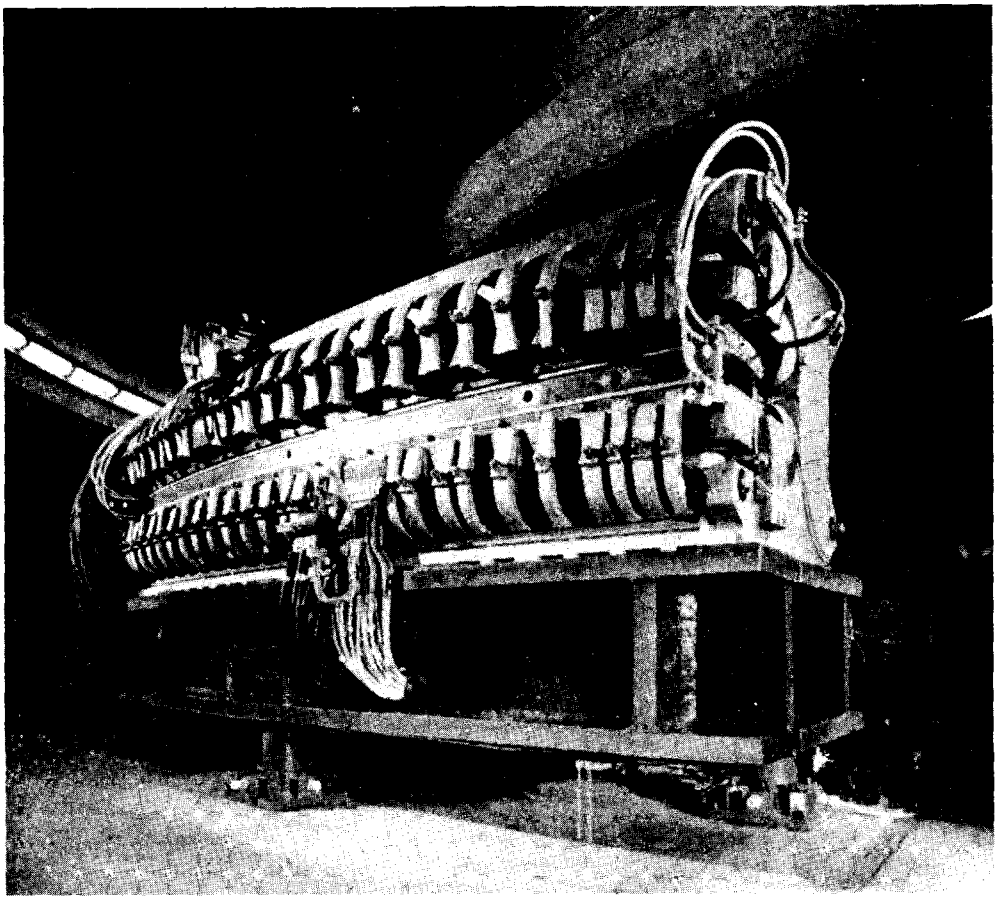

Fig. 1. Magnet semi-octant.

and 1.15. Each magnet weighs 40 t and contains 47 laminated yoke blocks (Fig. 3) and 94 separate pole piece blocks that were made wedge-shaped by machining after bonding to preserve a high-stacking factor and minimize azimuthal variations in B_z One advantage of the separable pole piece construction of the magnet was to allow production of the yokes to begin well in advance of the time when the pole piece design was frozen allowing greater flexibility both then, and in the future, should we want to change the shape of the pole pieces.

The pole tips being separable and spaced by stainless steel spacers that are accurate to 0.008 mm, are aligned with comparable accuracy. In order to obtain this precision of assembly quality control techniques were employed during the contour forming, stacking and curing of the yoke and pole piece laminations. The gap in the yoke laminations is accurate to within 0.05 mm around the machine and the parallelism of yoke gap base to the bottom of the yoke was maintained within 0.025 mm. The shims, spacer locations and gradient taper on the pole piece laminations were ground to an accuracy of 0.013 mm. The expected rms fractional deviation in the block to block value of the 7.77 cm vertical gap from tolerance build-up is 0.03% and the measured variation in the block to block value of B_z, at minimum field, over ten blocks in the prototype magnet is 0.1%. Variations in the average value of «n» over the same blocks, are about $\pm$ 3%.

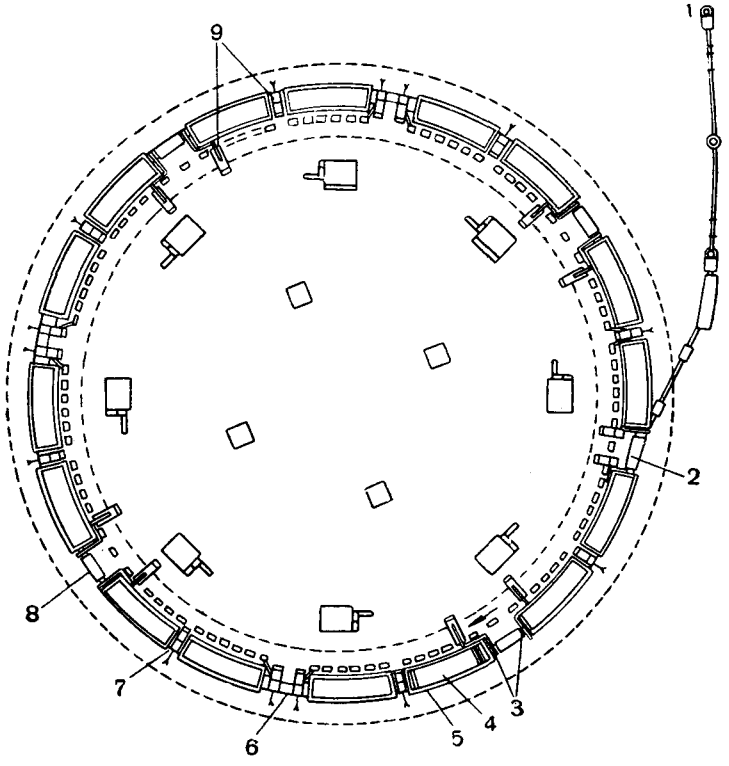

Fig. 2. Plan of magnet ring:
1 —from Van de Graaff generator; *2* — injector section; *3* — beam gate valves; *4* — magnet; *5* — box girder; *6* — 3 target sections; *7* — 8 beam-probe sections; *8* — 4RF sections; *9* — 24 pumping stations.

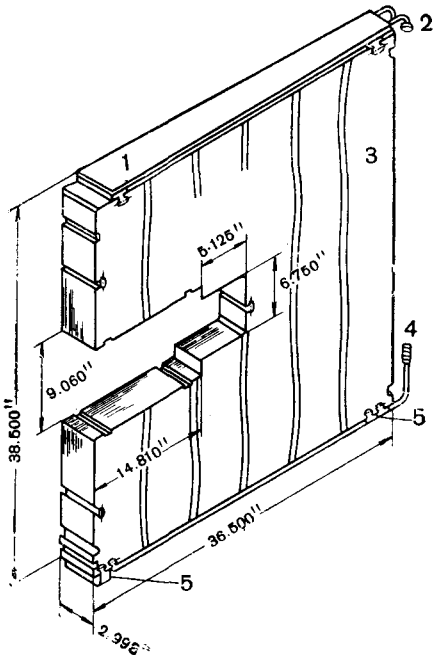

Fig. 3. Magnet yoke block:
1 — upper cooling tube pressure plate; *2* — upper cooling tubes; *3* — laminated magnet iron; *4* — lower cooling tubes; *5* — insulator pad.

2. MECHANICAL CHARACTERISTICS

The magnets rest on massive steel box girders which rest upon a rigid concrete foundation through three horizontally and vertically adjustable supports. Alignment of the yoke blocks is precise to 0.125 mm radially, and 0.02 mm vertically, and the surface upon which the pole tips rest was levelled to within 0.05 mrad.

The bonding of both the yoke and pole piece blocks was accomplished by eddy current heating techniques so that internal temperature differences would not exceed 10° C at the curing temperature of 200° C. A flexible bonding resin was used to minimize deleterious effects of strains in the magnet iron and the fixtures were designed to preserve lamination alignment during thermal expansion and contraction. The tolerance on block thickness is ± 0.1% and on block weight is ± 0.5%. The yoke blocks contain the seats for all pole piece, coil and vacuum chamber clamping devices (Fig. 4) and each clamp has a spring incorporated into it so that the clamping forces will remain relatively constant both during thermal expansion and contraction and after long-term compression of the asbestos-sheet-packing insulation which was used throughout because of its resistance to radiation. The yoke blocks are azimuthally clamped (Fig. 5) by two 7 cm steel end plates drawn together by stainless steel tie-bands. Azimuthal clamping of the pole piece blocks is accomplished in similar fashion using special melamine-glass end plates. Vertical clamping of the pole pieces is accomplished by two 1.0 cm by 2.5 cm pneumatic tubes that operate at 60 atmospheres.

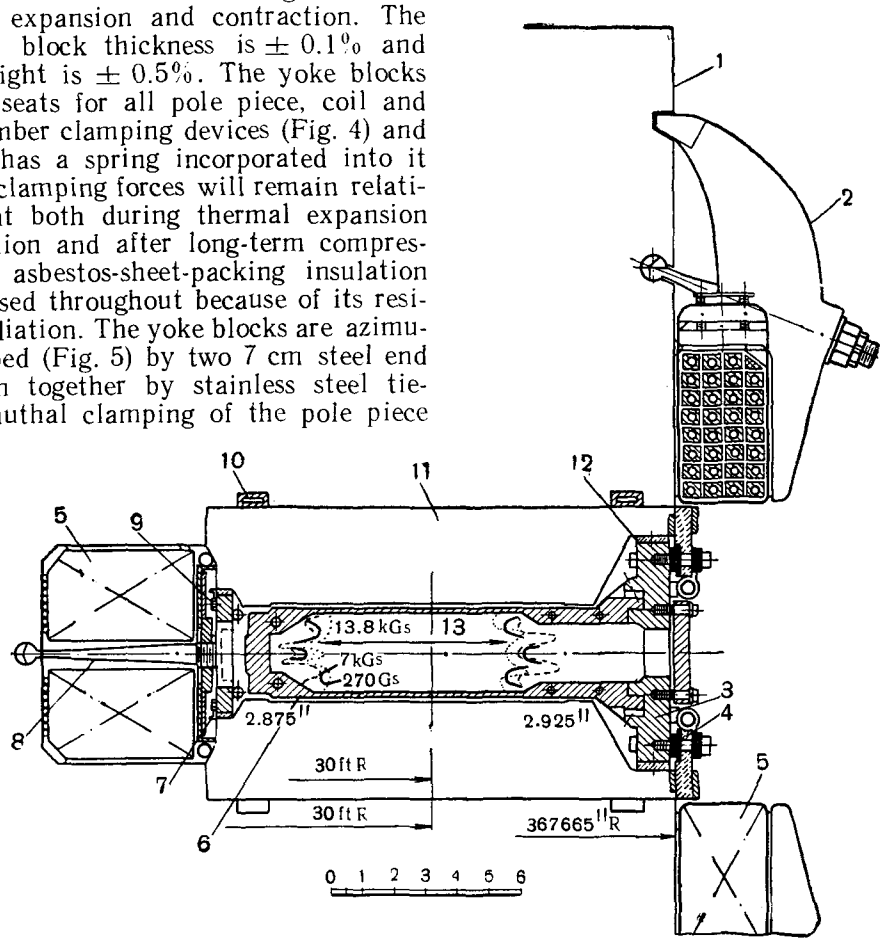

Fig. 4. Magnet cross-section showing coil clamps:
1 — magnet yoke block assembly; *2* — radial clamp assembly; *3* — front spacer and vacuum chamber assembly; *4* — pressure strip assembly; *5* — main magnet coil assembly; *6* — correction coils; *7* — ceramic insulator-rear; *8* — inside coil clamp assembly; *9* — back spacer assembly; *10* — pneumatic pressure hose; *11* — pole tip block assembly; *12* — ceramic insulator-front; *13* — extent of good «N» region.

3. COILS

The coils for the magnets are designed so that they conform very closely to the outline of the magnet and have a minimum clearance at the yoke pole piece interface. This, and the practice of locating power and water inlets and outlets to the coils, above and below the median plane, near the center of the magnets rather than at the ends, contributed to good confinement of the field in the magnet gap and to the minimization of stray fields. The coil insulation contains a high percentage of mica and glass for radiation resistance. The coils were wrapped with this glass-mica-tape and cured as a unit with an epoxy mixture that had been found satisfactory after radiation tests were analyzed. The coils are small enough to be handled by relatively simple fixturer and can be replaced, if the need arises, in about two weeks. The exci-

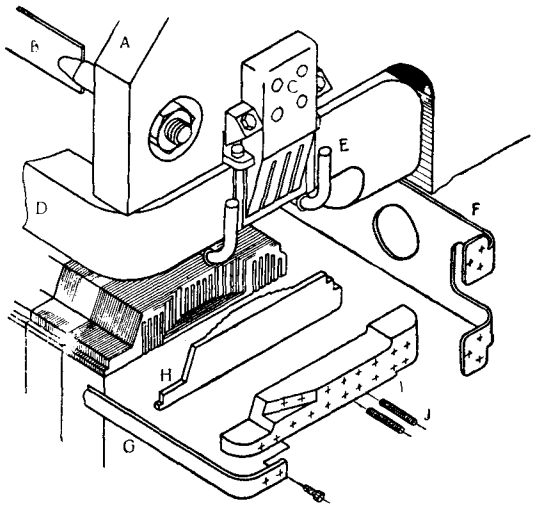

Fig. 5. End of magnet showing design of clamps:

A — 7 cm steel yoke block clamping plate; *B* — stainless steel tie band; *C* — end coil clamp; D — magnet coil; *E* — pheumatic pole tip clamping tube; *F* and *G* — pole tip clamping tie bands; *H* and *I* — melamine-glass pole tip clamping plates; *J* — pressure screws.

ting coils for each magnet operate at 1400 A (peak) and 8000 V (peak) from a resonant energy storage system of capacitors and a 16 section air-core inductance. The power is provided by rotating machinery with adjustable speed to maintain resonance. Regulation of the dc and ac components of the magnet current hold the minimum field constant to $\pm$ 0.3%.

4. MAGNET IRON

The steel used for both the yoke and pole piece blocks is Armco «A-6» Silicon Transformer Steel made to slightly more rigid specifications. We chose a lamination thickness of 0.64 mm as a good compromise between a high stacking-factor and the effects of eddy currents from our 19 cps field. (Our average stacking factor is about 0.93). Specifications on coercive force, low field permeability (we inject 10 Gs above the minimum field), and high field permeability were checked by measuring samples from the 140 ingots (seven heats) according to standard ASTM techniques. This steel is hot-rolled and has approximately the same permeability both parallel to and perpendicular to the applied field. At one time, we contemplated using a grain-oriented steel for the pole pieces, which had higher permeability than the «A-6» iron parallel to the applied field thereby reducing, in principle, the amount of field correction required at the peak field. These grain-oriented pole pieces, however, had very low permeability perpendicular to the applied field so that the pole clamping slots in the yoke blocks caused large bumps in the field.

The iron sample measurements and the production process itself were evaluated in order to develop a proper procedure for shuffling the iron sheets. The shuffling procedure developed was, in fact, not a random shuffling procedure but a method of averaging cyclic variations so that residual differences between blocks is minimal. Consequently, magnet yoke and pole piece blocks contain steel from all seven heats, 20 different ingots, and four «rolling packs» of twelve laminations each from the top fifth of ingots, the second fifth of ingots, etc. In order to accomplish this, shuffling was postponed until all the steel was produced and the ingots ordered so as to maximize the effect of the plan and minimize losses. A further refinement was to stack and cure the blocks in the same sequence as they were punched and then distribute them on the ring so that deleterious effects from the variations in the stamping and curing process were minimized. The first block was placed on magnet one, the second on magnet nine, and the third on magnet five, the fourth on magnet thirteen, etc.

5. MODEL STUDIES

We realized from the outset that in order to maintain our tolerances on B_z, «*n*» and median plane in this small an aperture (6.1 $\times$ 16.5 cm) for a weak focussing machine, extensive model studies and magnetic measurements both on, and off the median plane, would be required. We took the approach that the design of the magnet iron and the precision of fabrication should be adequate to obviate the need for extensive electrical field corrections. During the design stage, four models were built; a one-quarter scale model, a one-third scale model, a prototype magnet and a prototype magnet made from production parts. The one-quarter scale model magnet was used to develop the basic C-shape structure of the yoke blocks and a first approximation to the shape of the pole pieces including the location and approximate height of the shims and the angles which the pole edges make with the yoke. The one-third scale model was first used to fix the final contour of the yoke blocks including all the

notches and slots to be used for clamping seats so that the yoke laminations could be ordered early. The majority of the one-third scale work thereafter was devoted to the development of the pole piece contour including testing our first attempts at crenelation design; adding steel to the pole pieces to compensate for the bumps produced by the clamping slots in the yoke; optimization of the size of the back gap between the yoke and pole pieces to minimize the effects of the remanent field gradient and the selection of pole piece spacer locations such that ample room for target manipulation was provided within the confines of the magnet's vacuum chamber.

blem, we chose a method of slitting regular pole piece laminations so that, in effect, the end pole pieces are cross-laminated (Fig. 8). This choice allowed us the luxury of having square ends on the magnet permitting us to shorten each magnet by 8 cm giving a 10% increase in the length of the experimental straight sections.

6. MAGNETIC FIELD MEASUREMENTS

We measured the field gradients at injection fields using paramagnetic electron resonance in NH_3—Na. One probe, tuned to the injection field of 270 Gs (730 MHz), was kept at the cen-

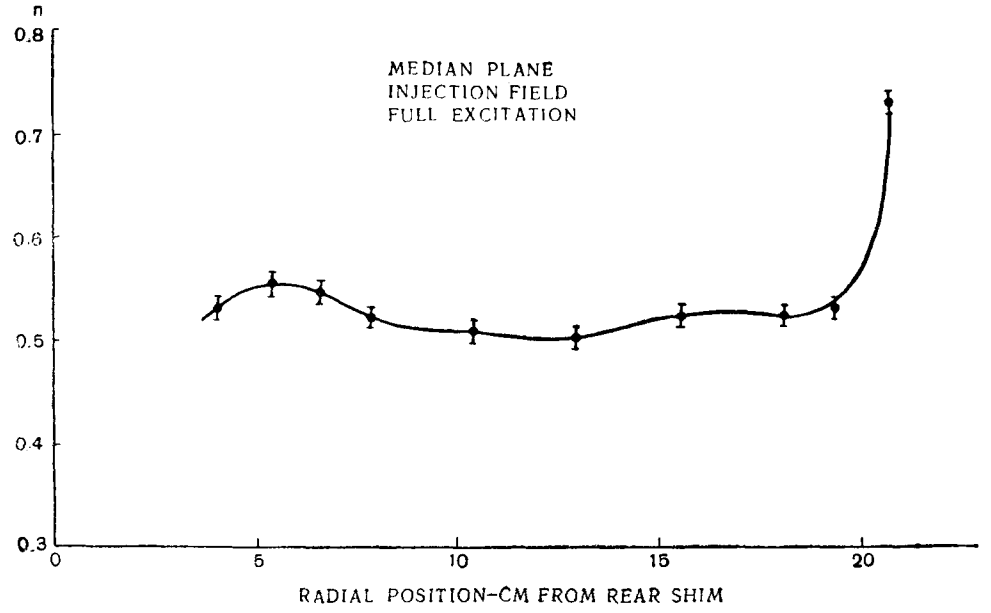

Fig. 6. «n» versus r at the injection field of 270 Gs.

Magnetic tests upon which the final pole piece design was based were performed on a prototype magnet, full scale in cross-section but one-third the length of a synchrotron magnet semi-octant. It was excited with a biased sine wave exactly like that which is used in operation of the synchrotron, in order to avoid spurious dependence of field shape upon the field program. It is interesting to note that when first constructed with standard pole pieces the end of the prototype magnet overheated to such an extent that it was obvious that the eddy currents produced in these end pole pieces would certainly cause undesirable magnetic end effects. Of the various possible solutions to this problem, we chose a method of slitting regular pole piece laminations so that, in effect, the end pole pieces are cross-laminated (Fig. 8). This choice allowed us the luxury of having square ends on the magnet permitting us to shorten each magnet by 8 cm giving a 10% increase in the length of the experimental straight sections.

6. MAGNETIC FIELD MEASUREMENTS

We measured the field gradients at injection fields using paramagnetic electron resonance in NH_3—Na. One probe, tuned to the injection field of 270 Gs (730 MHz), was kept at the center of the gap. The aperture was scanned by a second probe tuned so that its resonance signal was time coincident with that of the first. The resulting data on B as a function of radius and distance from the median plane had to be differentiated to obtain the gradient, resulting in rather large errors as shown in Fig. 6. The height of the shims at the pole edges and the gap between the back of the pole and the yoke was adjusted to maximize the useful aperture at injection. The first vacuum chamber models which were tried had a profound effect upon the injection field shape, caused by the finite magnetic susceptibility of the stainless steel parts. An alloy of 70 Cu—30 Ni was found with

a $(\mu-1) \leqslant 0.002$ which made the vacuum chamber magnetically inert.

Automatically recorded plots of «*n*» vs *B* were made by a computer which integrated the output from a line quadruple field gradient coil which averaged over an 8 cm length of the magnet. The constants of integration were manually inserted using data from the injection field measurements. The coil was proportioned to eliminate its octopole moment to give accurate point values of the gradient although the components of the coil had a 1 cm spacing. At intermediate fields, as expected, the field shape depended purely on geometrical factors. The pole pieces were flat within a few microns giving a good field shape even close to the poles.

Above 11 kGs, the uncorrected field shape deteriorated rapidly, due to saturation of the corners of the poles. Following the work of H. Bruck (Saclay) [2] this was compensated by the saturation of the ridges remaining between grooves in the pole faces (crenelation). We adjusted the depth of the grooves by fitting the measured deviations of the field shape from optimum by a sum of harmonic functions and calculating from them the variation of magnetic potential at the pole face. The width of the grooves controlled the field dependence of the correction. Plots of «*n*» vs radius at the peak field, with and without crenelation are shown in Fig. 7.

We also made measurements on the prototype magnet to verify that the magnetic median surface was sufficiently close to the geometrical median plane. A plate of alumina ceramic with an optically flat surface was set parallel to the geometrical median plane and served as reference for all measurements. The first step was to position a 0.05 mm diameter permalloy wire on the geometrical median plane with its axis approximately parallel to the reference plate and excite it with a 100 kHz sine-wave magnetizing field. It was then adjusted until it was perpendicular to the magnet's field as shown by a null in the second harmonic (200 kHz) output from a pickup coil observed at the time of the minimum field. By reversing the wire, we eliminated systematic errors in the orientation of the wire relative to the reference plate. In order to extend the measurements to higher fields, a line dipole coil which averaged over a 10 cm length of magnet was mounted with its axis accurately parallel to the reference plate as determined by reversing

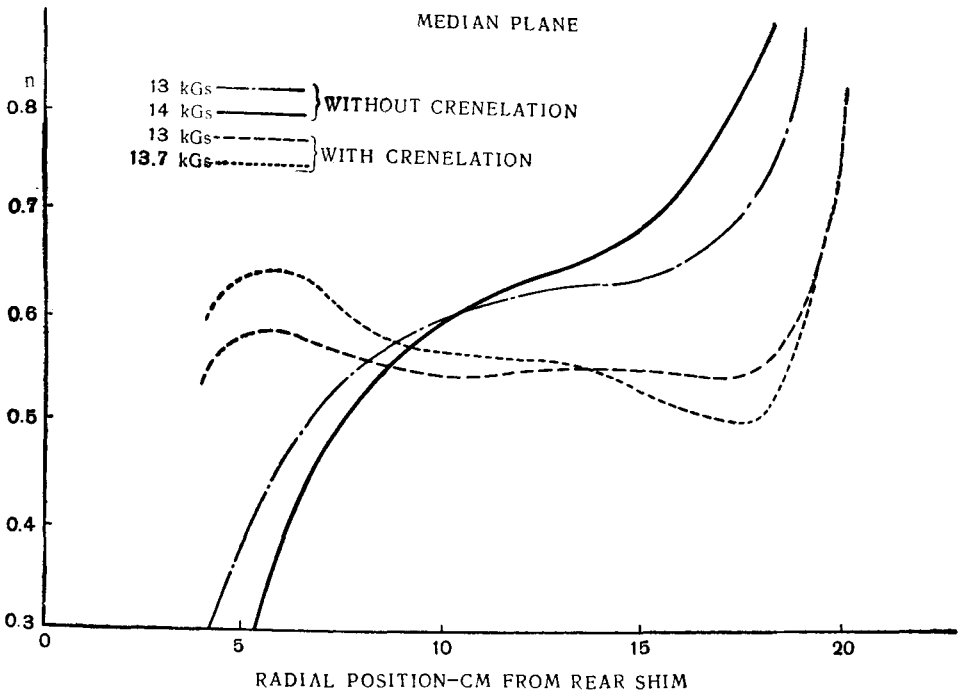

Fig. 7. «*n*» versus *r* on the median plane with plain and with crenelated pole pieces.

its direction. This coil was constructed with great care to avoid higher order errors. The accuracy of the measurements was limited by the accuracy with which the reference plate could be set, corresponding to an error of about 1 mm in the geometrical median plane location. The magnetic median surface was found to lie on the geometrical median plane within 2 mm except at the outside edge of the good «*n*» region where it drooped about 5 mm at low fields. This droop disappeared at fields above 1000 Gs. Tests with different pole pieces in the prototype magnet confirmed that the location of the magnetic median surface was controlled by mechanical factors so that we made no magnetic tests of the magnetic median surface in the completed synchrotron magnets. Subsequent studies with the proton beam have justified this decision.

Special attention was given to the focussing of the fringing fields at the ends of the magnets, as the Princeton-Pennsylvania Synchrotron has a relatively large number of straight sections for a weak focussing synchrotron. The measurements were made using a long coil (Fig. 8) which integrated from a region inside the magnet where the field was known to be essentially two dimensional to a point in the straight section where the field was negligible. The output from this coil was electrically subtracted from the output of a short coil mounted on the end which extended into the magnet. The data consisted of the distances the long coil extended into the magnet to null the integrated differential output from the two coils. The output of the electronic integrater was observed on an oscilloscope (Fig. 9) at a definite phase of the magnetic field variation, and the axial position of the coil adjusted so that the output at that phase was not changed when the coil was inverted. The outputs from the coils cancelled well enough to avoid overloading the electronic integrator which was sufficiently stable to permit measurements at the injection field. To make the coil large enough to provide this sensitivity, yet with accuracy in the derived radial gradients both coils were proportioned like one-half of an ideal line quadrupole, and the points were taken with the proper spacing. Mockups of the several types of straight secti-

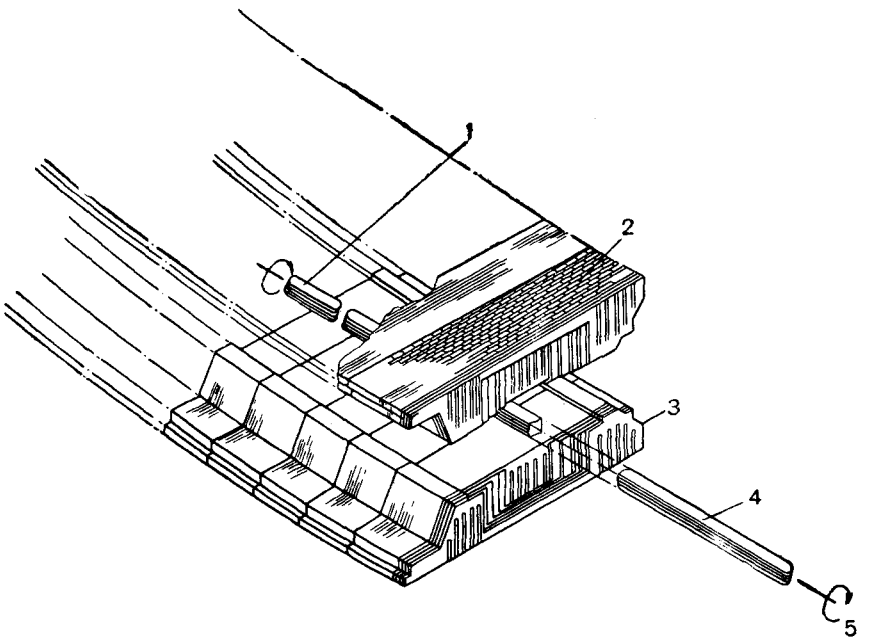

Fig. 8. Arrangement used to measure the fields at magnet ends. The long coil gave the integral through the fringe-field which was compared with the internal field given by the short coil. The shim plates corrected for field fall-off at the corners:
1 — short coil; *2* — slitted laminations; *3* — end field correction plate; *4* — long coil; *5* — rotation axis.

on hardware were mounted at the end of the prototype magnet to evaluate possible eddy current effects or magnetic shielding. The effective length of the magnet was found to be affected by certain of this hardware, but the focussing was to a good approximation independent of it. The field was found to fall off rather badly at the corners, but this was corrected with shim plates placed on the ends of the pole pieces (Fig. 8).

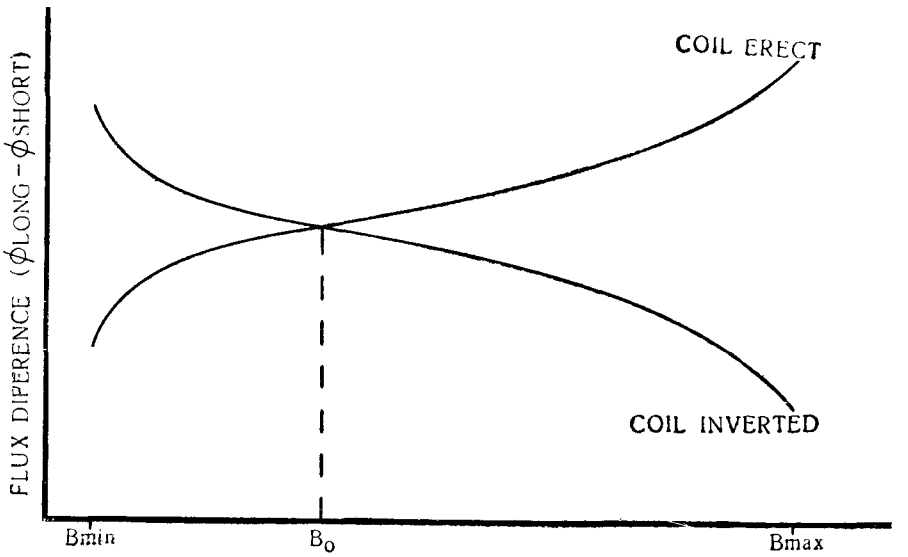

Fig. 9. The difference in flux in the long and short coils used for end field measurements plotted against B in the magnet, as it was observed on an oscilloscope. The setting corresponds to a measurement at the field B_0.

7. SUMMARY

Eventually, we found that with careful attention to: (a) «on and off» median plane measurements; (b) the design of crenelated pole pieces; (c) the maintenance of rigid tolerances in mechanical fabrication and assembly; (d) the use of contour grinding of the important pole piece surfaces rather than punching; and (e) strict adherence to our shuffling plan, we were able to make magnets with essentially the same good «n» region 6.1 × 16.5 cm at all fields, a magnetic median surface in close agreement with the geometric median plane and low field block-to-block variations in B_z of about 0.1% — without correction. We did provide minimum-field correction coils for «n» and median plane and use the «n» coils to insure avoidance of the $n = 0.5$ resonance. A correction, provided by control room operated shunts across each magnet, of about 0.3 per cent peak to peak in the magnet to magnet value of $B_{\min}$, is required for optimum injection conditions.

The magnet has been operated at full power for over 2000 h and runs quietly with the largest amplitude of vibration being 0.08 mm. With proper aiming of the injected beam and the application of the $B_{\min}$ corrections, we can reliably inject nine turns of 3 MeV protons with essentially no radial betatron oscillations and vertical excursions no greater than 0.5 cm from the geometric median plane.

ACKNOWLEDGEMENTS

Of the many people whose hard work contributed so much to the program described in this paper, the following deserve special mention: M. Awschalom, M. V. Isaila, C. R. Sun, and E. P. Tomlinson for their work on the magnetic field measurements. D. L. Collins, S. Hochman, J. H. Kellock, M. Scheibner, T. C. Tang and K. E. Wright for their work on the mechanical design and construction. E. de Haas and S. Waaben for their work on the magnet power supply.

REFERENCES

1. A l l e n H. L. et al. See this edition, p. 161.
2. B r u c k H. et al. In: Proceedings of the CERN Symposium on High Energy Accelerators and Pion Physics (Geneva, 1956), v. I, pp. 330–338.